Supporting Information

Two-dimensional MX_2Y_4 systems: Ultrahigh carrier transport and excellent hydrogen evolution reaction performances

Kai Ren[1,*], Huabing Shu[2], Ke Wang[3] and Huasong Qin[4,*]

[1]School of Mechanical and Electronic Engineering, Nanjing Forestry University, Nanjing 211189, China
[2]School of Science, Jiangsu University of Science and Technology, Zhenjiang 212001, China
[3]School of Automation, Xi'an University of Posts & Telecommunications, Shaanxi, 710121, China
[4]Laboratory for Multiscale Mechanics and Medical Science SV LAB, School of Aerospace Xi'an Jiaotong University, Xi'an 710049, China
E-mail: kairen@njfu.edu.cn (Kai Ren), huasongqin@xjtu.edu.cn (Huasong Qin)

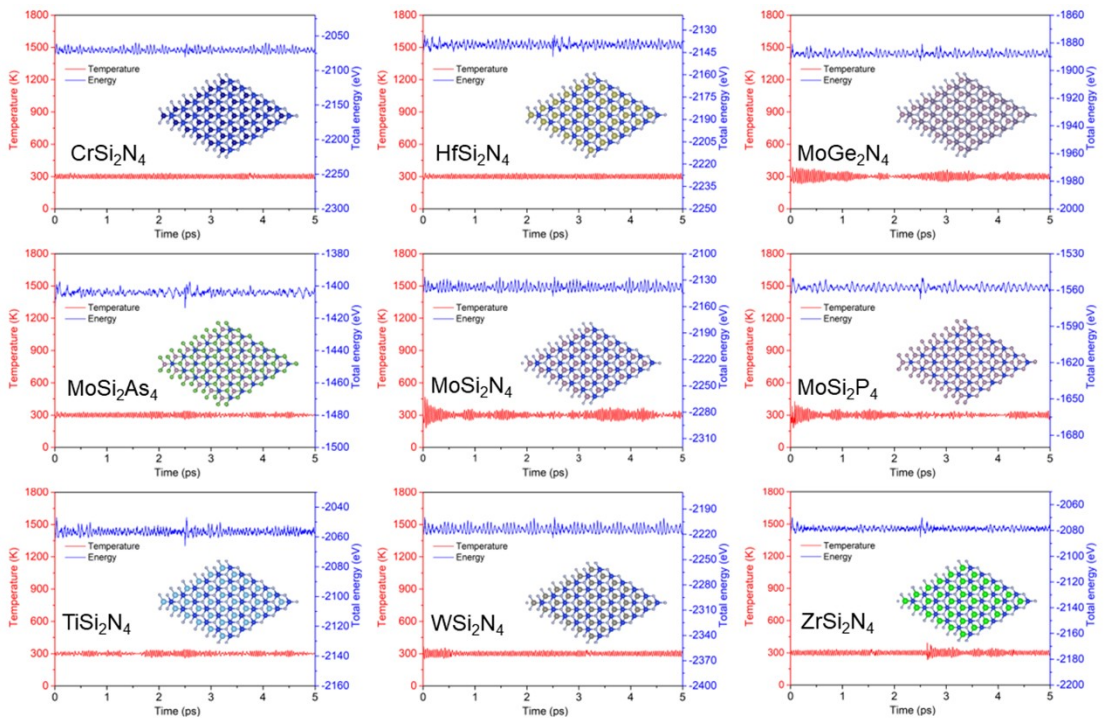

Fig. S1. The obtained temperature fluctuation and the total energy of the MX_2Y_4 monolayer during the AIMD simulation, the insets are the atomic structure after 5 ps at 300 K.

Table S1. The calculated elastic constants of these MX_2Y_4 monolayer.

Monolayer	C_{11}	C_{22}	C_{12}	C_{66}
$CrSi_2N_4$	203.90	203.90	62.13	0.13
$HfSi_2N_4$	180.39	180.39	59.03	–0.04
$MoGe_2N_4$	172.20	172.20	56.11	0.16
$MoSi_2As_4$	72.32	72.32	21.08	–0.02
$MoSi_2N_4$	213.81	213.81	61.38	0.14
$MoSi_2P_4$	86.28	86.28	22.79	0.09
$TiSi_2N_4$	192.78	192.78	60.41	0.11
WSi_2N_4	222.65	222.65	62.28	–0.05

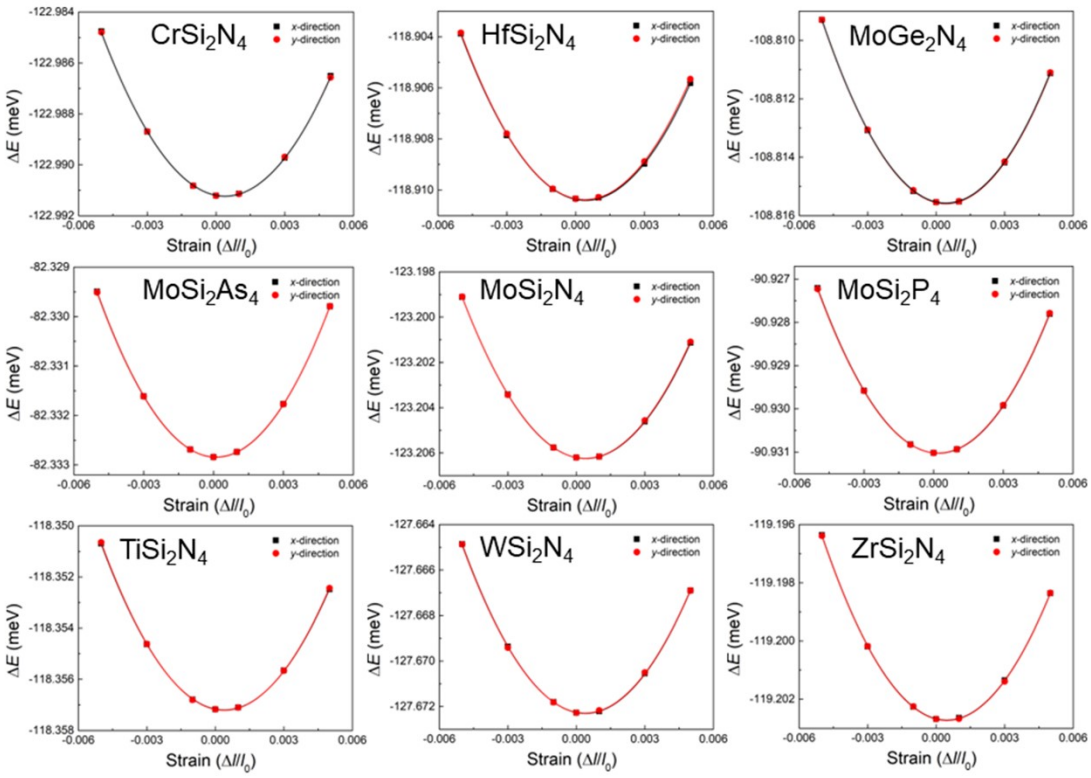

Fig. S2. The obtained energy difference of the MX_2Y_4 monolayer under the external strain.

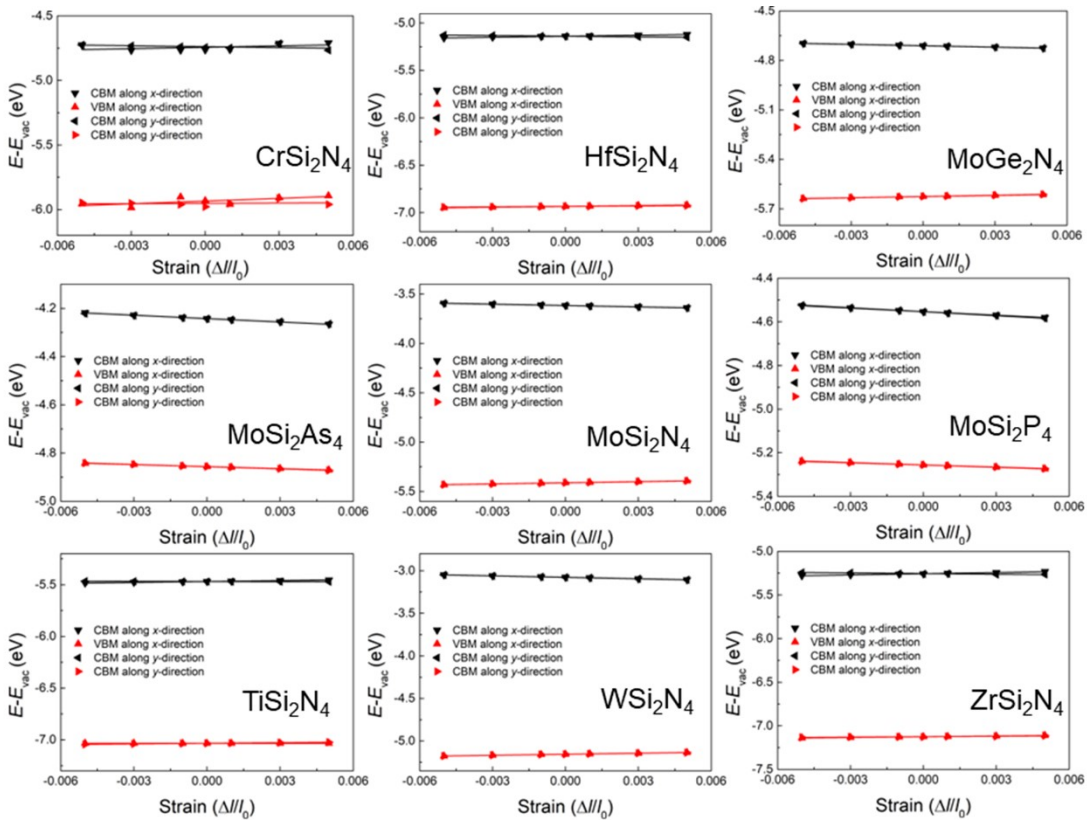

Fig. S3. The calculated band edge position difference of the MX_2Y_4 monolayer under the external strain.

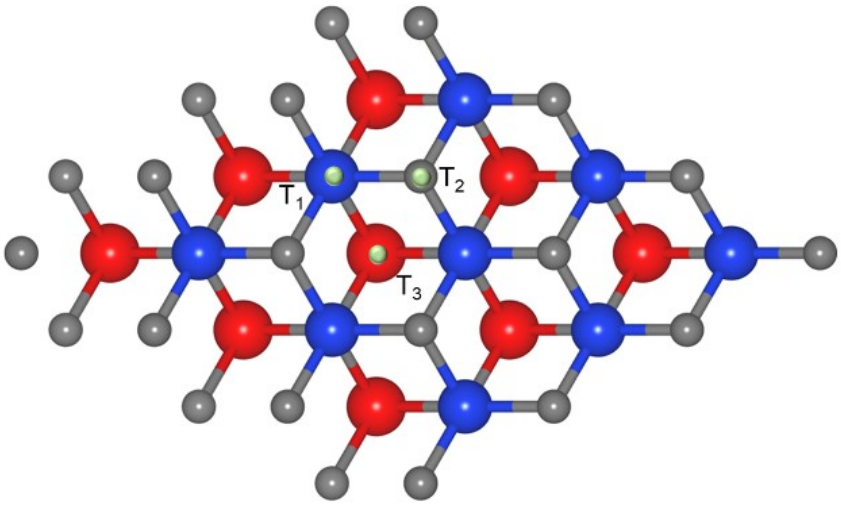

Fig. S4. The top and side views of the most stable adsorption configuration for the MX_2Y_4 monolayer. The red, blue and gray balls represent the M, X and Y atoms, respectively.

Table S2 The PBE calculated effective mass (m, m_e), deformation potential constant (E, eV), elastic modulus (C, N/m) and the carrier mobility (μ, $cm^2 \cdot V^{-1} \cdot s^{-1}$) for the hole (h) and the electron (e) of the MX_2Y_4 monolayer along the transport directions.

materials	direction	carrier	m	E	C	μ
$CrSi_2N_4$	x	e^-	1.84	1.59	503	826
		h^+	−3.50	2.53		85
	y	e^-	1.88	−4.08	511	125
		h^+	−4.04	2.53		75
$HfSi_2N_4$	x	e^-	1.86	3.59	451	206
		h^+	−0.55	2.87		1182
	y	e^-	0.90	−2.37	447	966
		h^+	−2.63	1.69		706
$MoGe_2N_4$	x	e^-	0.79	−2.82	428	1226
		h^+	−0.95	2.34		1248
	y	e^-	0.79	−2.83	428	1225
		h^+	−0.94	2.56		1045
$MoSi_2As_4$	x	e^-	0.54	−4.69	181	386
		h^+	−0.42	−2.77		1874
	y	e^-	0.57	−4.25	180	446
		h^+	−0.44	−3.02		1476
$MoSi_2N_4$	x	e^-	0.45	−4.62	531	1730
		h^+	−1.75	3.8		172
	y	e^-	0.46	−4.61	533	1721
		h^+	−1.73	3.8		174
$MoSi_2P_4$	x	e^-	0.33	−5.43	216	932
		h^+	−0.35	−3.59		1889
	y	e^-	0.34	−6.01	215	736
		h^+	−0.37	−3.26		2169
$TiSi_2N_4$	x	e^-	2.69	2.95	480	141
		h^+	−5.14	−0.6		1695
	y	e^-	1.59	−0.45	484	10370
		h^+	−0.92	2.05		815
WSi_2N_4	x	e^-	0.34	−5.7	557	2172
		h^+	−1.53	4.05		205
	y	e^-	0.34	−5.7	556	2162
		h^+	−1.55	4.05		203
$ZrSi_2N_4$	x	e^-	1.83	4.44	427	93
		h^+	−3.84	2.67		76
	y	e^-	1.82	−2.71	427	250
		h^+	−2.25	1.15		694

Table S3 The calculated most favorable adsorption sites and the Gibbs free energy of the H adsorbed MX_2Y_4 monolayer system.

Monolayer	Site	Gibbs free energy (eV)
$CrSi_2N_4$	T_2	4.158
$HfSi_2N_4$	T_3	0.228
$MoGe_2N_4$	T_2	1.269
$MoSi_2As_4$	T_3	1.481
$MoSi_2N_4$	T_2	2.326
$MoSi_2P_4$	T_1	1.468
$TiSi_2N_4$	T_1	0.078
WSi_2N_4	T_2	2.576
$ZrSi_2N_4$	T_1	−0.035